Electrocatalytic Properties of meso - Perfluorinated Metallo Corroles for the Reduction of CO 2

Chanjuan Zhang, Paul-gabriel Julliard, Diana Dragoe, Ally Aukauloo, Gabriel Canard

EurJIC
European Journal of Inorganic Chemistry

Research Article
doi.org/10.1002/ejic.202400318

Chemistry Europe
European Chemical Societies Publishing

www.eurjic.org

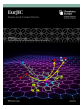

Electrocatalytic Properties of *meso*- Perfluorinated Metallo Corroles for the Reduction of CO_2

Chanjuan Zhang,[a] Paul-Gabriel Julliard,[b] Diana Dragoe,[a] Ally Aukauloo,*[a, c] and Gabriel Canard*[b]

Tetrapyrrolic containing metal complexes are among the most efficient molecular catalysts for the CO_2 reduction. Metalloporphyrins and phthalocyanines are currently under investigations and their catalytic properties are among the best molecular catalysts. Corrole, a contracted tetrapyrrolic macrocycle has been also used to design molecular for the CO_2 reduction. The electrochemical activity towards CO_2 reduction can rival those of their porphyrin analogues. However, the catalytic activity of the metallocorrole is initiated at the corresponding $M^{II/I}$ couple. Accordingly, a catalytic current in presence of CO_2 with cobalt corrole appears when the Co^{I} species is generated. We have designed an electron deficient A_2B corrole holding two $-CF_3$ groups and a benzonitrile in the *meso* positions and its cobalt complex (**1**). We reasoned that these groups could shuffle the redox potentials to reach the M(I) oxidation states at more positive values thereby lowering the overpotential for the catalytic CO_2 reduction. Our results clearly show that catalyst **1** when adsorbed on a carbon electrode, shows the most favourable catalytic performance for CO production, achieving an efficiency of 85% with a current density of $-1.5\ mA\,cm^{-2}$ at -1.0 V *vs* NHE. The current densities of controlled potential electrolysis with increasing amount of $KHCO_3$, were found to increase more than one order of magnitude with the formation of MeOH.

Introduction

The climate neutrality of *e*Fuels relies on the use of cheap electricity produced from renewable sources to perform highly energy consuming processes for converting small molecules such as CO_2, H_2O and N_2 to chemical fuels or commodities.[1] Among the different challenges, the electrocatalytic conversion of CO_2 to reduced forms of carbon is actively being pursued as a sustainable way to produce a fuel.[2] Many catalytic materials are currently under investigation with the target to perform such transformation on a massive scale.[3] The design of molecular based catalysts that can replicate the catalytic power of the active sites of the six grand families of enzymes that manage the multi GTon chemistry of CO_2 in our biosphere may indeed lead to the discovery of highly cost-efficient catalysts.[4] Tetrapyrrolic containing metal complexes are among the most efficient molecular catalysts for the reduction CO_2. Indeed, metallo-porphyrins and phthalocyanines can catalyze the reduction of CO_2 to a variety of reduced forms from CO,[4b,5] HCOOH,[6] CH_3OH[7] to CH_4[8] with high turnover frequencies and numbers at moderate overpotentials. Their catalytic properties are being constantly boosted following the implementation of chemical functionalities inspired from the active sites of enzymes.[4a,5,9] Corrole, another tetrapyrrolic macrocycle has also been used as ligands to develop catalysts for the CO_2 reduction.[10] The macrocycle differs mainly from the smaller size of the N_4 coordinating cavity with respect of porphyrin and phthalocyanine and is also a trianionic ligand thereby more prone to stabilize metal ions in their high oxidation states. However, as in the case of porphyrins, corroles also participate in the redox properties of their corresponding metallo-complexes. Neta, Fujita, Gross, and collaborators have reported the first electrocatalytic behavior of a series of cobalt and iron corroles for the CO_2 reduction in homogeneous medium.[10b] As expected, the trianionic nature corrole shifted the reduction potentials of the central metal ion to more negative values in comparison with their porphyrin analogues. In presence of CO_2 the metallocorroles could reduce CO_2 to CO at the M^{+I} oxidation state.[4a,11] A major finding in the CO_2RR using metallocorroles as catalysts was reported by Roy, Schöfberger and coworkers where the authors have found that when deposited on a carbon paper electrode cobalt corroles could produce a variety of highly reduced forms of carbon such as methanol and ethanol at quite low overpotentials at pH 6.[10a] Low amount of acetic acid was also evidenced. Such a finding was unprecedented and draw a considerable attention on the corrole chemistry for the development of molecular catalysts for the

[a] C. Zhang, D. Dragoe, A. Aukauloo
Université Paris-Saclay, CNRS, Institut de Chimie Moléculaire et des Matériaux d'Orsay, 91400 Orsay, France
E-mail: ally.aukauloo@universite-paris-saclay.fr

[b] P.-G. Julliard, G. Canard
Aix Marseille Univ, CNRS, CINAM, UMR 7325, Centre Interdisciplinaire de Nanoscience de Marseille, Campus de Luminy, 13288 Marseille Cedex 09, France
E-mail: gabriel.canard@univ-amu.fr

[c] A. Aukauloo
Université Paris-Saclay, CEA, Institute for Integrative Biology of the Cell (I2BC), 91198 Gif-sur-Yvette, France

Supporting information for this article is available on the WWW under https://doi.org/10.1002/ejic.202400318

Research Article
doi.org/10.1002/ejic.202400318

CO_2 reduction. The same teams later discovered that manganese corroles were also highly efficient for the selective CO_2 reduction to acetic acid when immobilized on carbon paper electrode.[12] Both of these studies were supported by a thorough DFT analysis and in the first case a formic acid pathway, while in the second case an oxalate intermediate was proposed. The remarkable catalytic activity and selectivity of these corrole based catalysts were attributed to the presence of the perfluoro phenyl groups in the *meso* positions that helped to shift the potentials of the cathodic processes to more positive values. An important feature in the design of these catalysts is the presence of the S-PEG (7)-OMe introduced in the *para* positions of the phenyl rings. These groups would help in a better anchorage and distribution of the molecular catalysts on the surface of the carbon electrode. When controlled experiments were done with the three *meso*-C_6F_5 groups of the cobalt corrole catalyst only traces of ethanol were detected. Henceforth, one can postulate that the PEG groups may also intervene in stabilizing reactive intermediates upon catalysis that would lead to such an outstanding catalytic reactivity, albeit there is no experimental proof for such a proposal and furthermore have not been considered in the theoretical analyses for backing the experimental findings. Gross and coworkers recently described the reactivity of the superstructured cobalt and iron corrole complexes holding a napthol group.[13] The authors found that the catalytic efficiency of the corrole complex was enhanced in comparison with the three *meso*-C_6F_5 groups of the cobalt corrole.

We have been interested in examining the electrocatalytic properties of an electron deficient A_2B corrole holding two $-CF_3$ groups and a cyanobenzene in the *meso* positions. We reasoned that these groups could shuffle the redox potentials to reach the M(I) oxidation states at more positive values thereby lowering the overpotential for the catalytic CO_2 reduction. Our results clearly show that when adsorbed on a carbon electrode no reduced forms of carbon other than CO was detected for the cobalt catalyst (**1**) (Scheme 1) and in the case of the manganese corrole (**3**), only the HER was undergoing. Controlled experiments with the three substituted *meso*-C_6F_5 cobalt corrole (**2**) also indicated that only CO and methanol was formed while the corresponding manganese complex (**3**) was found to catalyze only the HER under our experimental conditions.

Results and Discussion

Complexes **2** and **3** were prepared from trispentafluorophenylcorrole according to published protocols.[14] The synthesis of design A_2B corrole holding two $-CF_3$ groups and a benzonitrile in the *meso* positions was realized following a two-steps reported procedure as depicted in Scheme 2 and the experimental details can be found in the Supplementary Information.[15] The cobalt complex **1** was prepared upon metalation of the proligand with cobalt(II) acetate in presence of triphenylphosphine.

Crystals of **1** of sufficient quality for the X-ray diffraction analysis were obtained. The coordination scheme of the cobalt ion can be described with four nitrogen atoms of the corrole coordinating cavity set in a trapezoidal disposition and a triphenylphosphine group in an axial position. The structural metrics of **1** are given in the SI. Figure 1.

Electrochemical Results

The cyclic voltammograms (CVs) of **1**, **2** and **3** in DMF under Ar and CO_2 atmosphere are illustrated in Figure 2 and Table 1. In an argon atmosphere, three reduction peaks are observed in

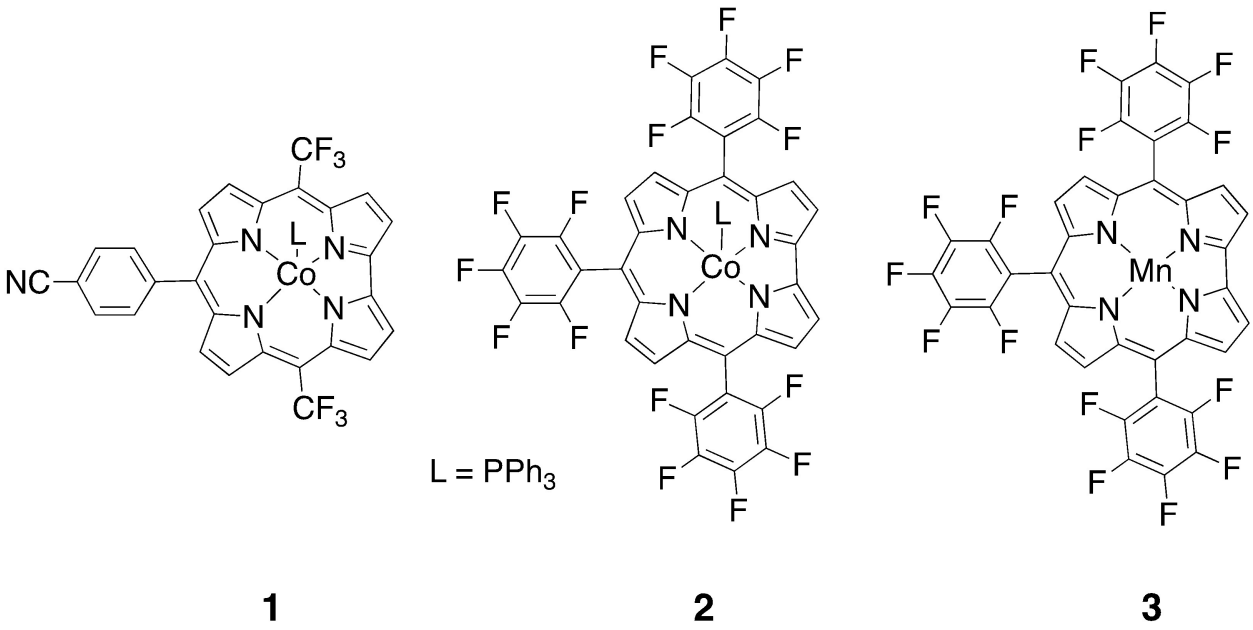

1 **2** **3**

Scheme 1. Complexes **1**, **2** and **3**.

Research Article
doi.org/10.1002/ejic.202400318

Chemistry Europe
European Chemical Societies Publishing

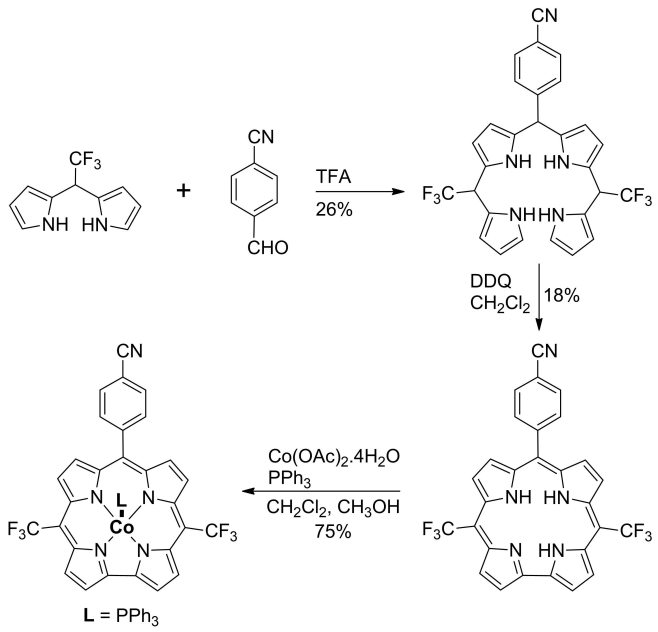

Scheme 2. Synthetic route for the obtention of the triphenylphosphino-Cobalt(III)-5,15-bis(trifluoromethyl)-10-(4-cyanophenyl)corrole (**1**).

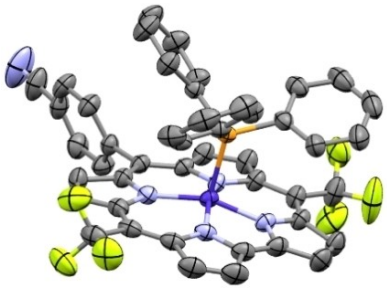

Figure 1. The X-ray structure of (**1**) (Hydrogen atoms are omitted for clarity).

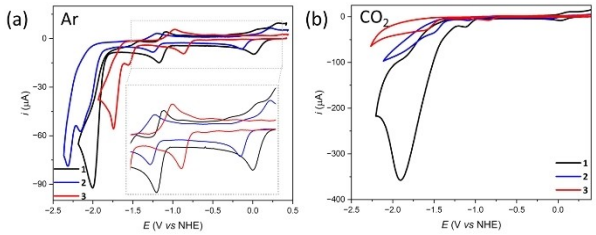

Figure 2. (a) CVs of 1 mM **1** (black), **2** (blue) and **3** (red) in DMF containing 0.1 M Nbu_4PF_6 under argon. (b) under CO_2 saturation with 5 M H_2O. Scan rate 0.1 V s^{-1}.

Table 1. Half-wave potentials for reduction of **1**, **2** and **3** in DMF.

Molecule	$E_{1/2}$ (V *vs* NHE)
1	0.02, −1.17, −2.0
2	−0.14, −1.25, −2.15, −2.31
3	−0.87, −1.56, −1.74

the CV of catalyst **1**. The first reduction, occurring irreversibly at E_{pc} = 0.02 V *vs* NHE, is likely associated with the $Co^{III/II}$ species and involves partial lost of the PPh_3 ligand, in agreement with the reported electrochemical property of cobalt corrole.[10b] This reduction is coupled with reoxidation events at E_{pa} = 0.07 V and 0.31 V. The second reduction, reversible at E_{pc} = −1.17 V, corresponds to $Co^{II/I}$. The final reduction peak, at −2.0 V, is likely attributable to multi-electron reduction of $-CF_3$ groups. For catalyst **2**, four reduction peaks are observed. The first reduction peak, occurring at E_{pc} = −0.14 V, is reversible and associated with $Co^{III/II}$, in contrast to reported results by Grodkowski and Neta.[10b] The second reduction ($Co^{II/I}$) occurs at −1.25 V, with a reversible reoxidation peak at E_{pa} = −1.20 V. The third and fourth reduction peaks, at −2.15 V and −2.31 V respectively, are irreversible and attributed to the multi-electron reduction of the substituted corrole macrocyle. It is noteworthy that we observed all reduction potentials of catalyst **2** to be slightly more negative than those of catalyst **1**. This difference can be assigned to the stronger electron withdrawing effect of the $-CF_3$ groups on catalyst **1**. Regarding catalyst **3**, three reduction peaks are observed at E_{pc} = −0.87 V, −1.56 V, and −1.74 V. In the cyclic voltammogram of manganese corrole **3** in DMF, only the first reduction peak is reversible, with a reoxidation peak at E_{pa} = −0.98 V, likely corresponding to the reduction of Mn^{III} to Mn^{II}. The second reduction, which takes place at −1.56 V, corresponds to the $Mn^{II/I}$ transition and exhibits irreversibility, consistent with the behavior observed in other reported manganese complexes.[16]

The electrocatalytic properties of the designed catalysts were investigated by conducting cyclic voltammetry (CV) experiments in DMF under a CO_2 atmosphere (Figure 2b). When comparing the performance of catalyst **1** under Ar with that under CO_2, a noticeable increase in current was observed at −1.25 V *vs.* NHE, where the formation of Co^{I} occurred in the presence of CO_2 in DMF (see Figure S1b). This observation indicates that Co^{I} serves as the active species for CO_2 activation, affirming that metallocorroles are capable to catalyze the transformation of CO_2 at the M^{+I} oxidation state. Furthermore, when H_2O was introduced as the proton source in DMF under a CO_2 atmosphere, catalyst (**1**) exhibited a significant increase in current, reaching up to 360 μA, thereby demonstrating its strong CO_2 catalytic performance (see Figure S1a). Compared to **1**, catalyst **2** displayed a notably lower current for CO_2 catalysis, as shown in Figure 2b and Figure S2. In contrast to some previously reported findings, no evident CO_2 catalysis was observed with catalyst **3**.[12]

To examine the catalytic efficiency for CO_2 electroreduction of the designed catalyst **1** and its comparison with known catalysts (**2**) and (**3**), they were immobilized on carbon paper with multi-wall carbon nanotubes, following the same preparation method as in previous studies.[5a,17] The controlled potential electrolysis for CO_2 electrolysis of CNT-**1** was conducted over a duration of 120 minutes in a CO_2-saturated 0.1 M $NaHCO_3$ aqueous solution, maintaining a stable current density of -1.5 mA cm^{-2} (Figure 3a). Gas product analysis via gas chromatography (GC) during controlled potential electrolysis indicated that CO predominated as the major product, achieving a

Research Article
doi.org/10.1002/ejic.202400318

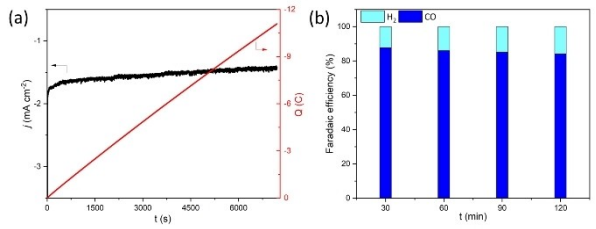

Figure 3. Controlled potential electrolysis using CNT-**1** electrode (10 mm×10 mm) at −1.0 V *vs* NHE in CO_2-saturated 0.1 M $NaHCO_3$ aqueous solution. a) i (black) and consumed charge (red) *vs* t, b) FE of CO (blue) and H_2 (cyan).

faradaic efficiency of approximately 85% over the 2 hour electrolysis period, as illustrated in Figure 3b. An identical electrolysis procedure was applied to CNT-**2**, resulting in a CO faradaic efficiency of approximately 80%, with a current density of −0.3 mA cm^{-2}, which was five times slower than that of CNT-**1**. Additionally, CNT-**3** underwent CO_2 electrolysis under the same condition as CNT-**1**, yet only hydrogen was detected by gas chromatography. Comparative analysis of the controlled potential electrolysis data from CNT-**1**, CNT-**2**, and CNT-**3** electrodes suggests that CNT-**1** demonstrated the most favourable catalytic performance for CO production, achieving an efficiency of 85% with a current density of −1.5 mA cm^{-2} at −1.0 V *vs* NHE. This outcome prompts us to focus our further investigations specifically on CNT-**1**.

Nuclear magnetic resonance (NMR) analysis of the electrolyte at −1.0 V in 0.1 M $NaHCO_3$ ruled out the formation of liquid products such as formate, formaldehyde, or methanol during the electrolysis. To go beyond, we aimed to optimize the electrochemical performance by reassessing the electrolyzer configuration. To achieve this, we conducted various electrolysis experiments using higher electrolyte concentrations (0.5 M, 1 M, and 3 M $KHCO_3$) in a CO_2-saturated aqueous solution at −1.4 V *vs* NHE. As shown in Figure 4, the current densities of controlled potential electrolysis of CNT-**1** in 0.5 M, 1.0 M, and 3.0 M $KHCO_3$ escalated to −9.7 mA cm^{-2}, −11.1 mA cm^{-2}, and −19.1 mA cm^{-2}, respectively, surpassing that observed in 0.1 M $NaHCO_3$ by more than one order of magnitude. Interestingly, the liquid product analysis via NMR revealed the presence of trace amounts of MeOH, with the highest selectivity recorded at

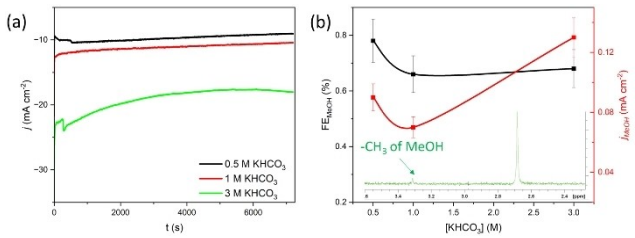

Figure 4. Controlled potential electrolysis using CNT-**1** electrode (10 mm×10 mm) at −1.4 V *vs* NHE in CO_2-saturated 0.5 M (black), 1.0 M (red), and 3.0 M (green) $KHCO_3$ aqueous solution. (a) j *vs* t, (b) FE_{MeOH} and j_{MeOH} *vs* [$KHCO_3$], the NMR of electrolyte was inserted to show the production of MeOH.

0.8% in 0.5 M $KHCO_3$. Notably, the highest partial current density for CO_2 reduction to MeOH was observed at −0.12 mA cm^{-2} in 3 M $KHCO_3$, which is four times higher than the reported partial MeOH production from CO_2 electroreduction with cobalt phthalocyanine,[7a] and the activities towards MeOH production can still be improved by the modification of the corrole ring.[18]

CNT-**1** electrodes were characterized by using solid UV/vis, FTIR, and XPS before and after electrolysis to monitor any chemical alteration of the adsorbed catalyst. In the solid UV/vis spectra (Figure S4), two Q-bands of CNT-**1** were identified at 567 nm and 671 nm, consistent with Q-bands observed in other reported cobalt corroles.[19] After electrolysis, these two Q-bands maintained a similar shape, indicating no marked structural changes occurred during the electrolysis process. Furthermore, Fourier-transform infrared spectroscopy (FTIR) analysis (Figure S5) confirmed the stability of the catalyst. The integrity of functional groups such as C≡N, C=C, C=N, C–F and Co–PPh_3 at 2228 cm^{-1}, 1604 cm^{-1}, 1345 cm^{-1}, 1257 cm^{-1}, and 850 cm^{-1} respectively, supported the conclusion that CNT-**1** did not suffer significant structural modifications during the electrolysis. X-ray photoelectron spectroscopy (XPS) spectra (Figure S5) conducted on the CNT-**1** electrode before and after electrolysis exhibited slight shift in binding energy for Co 2p, N1s, and F1s. A comparison between the Co2p core-level spectra of CNT-1 before and after electrolysis (Figure S6a) shows that some changes occur in the environment of a part of Co cations. The $Co2p_{3/2}$ component of the spin-orbit coupling doublet, located at 780.4 eV in the Co-corrole complex[10a] is shifted by 0.6 eV toward higher BE in the complex after electrolysis. This may come from the presence of different axial ligands on the cobalt center. As already observed for metallo-porphyrins or metallo-phthalocyanins where demetallation may occur at the surface of electrodes, we also noticed that during electrolysis a change in the N1s core-level spectra (Figure S6b).[20] The spectrum of CNT-**1** before electrolysis shows one main component located at 399.3 eV and corresponding to the metalated corrole[21] while a second component, centered at 400.7 eV, appears in CNT-**1** after electrolysis. This component can be attributed to C–NH[22] and suggests that part of Co-corrole gets demetalated during electrolysis.

We have shown herein that the electrocatalytic activity of cobalt corroles can be enhanced through the chemical nature of the substituents at the *meso* positions. The *meso*-substituted –CF_3 derivative boosted the electrocatalytic performance of cobalt containing catalyst for the reduction of CO_2 to CO with a remarkable $ip_{cat}/ip_0 = 24$. Heterogeneous catalysis with a modified carbon paper electrode also points to the formation of MeOH. Further studies are underway to understand the mechanism of formation of MeOH with the cobalt corrole catalyst **1**.

Acknowledgements

We are indebted to the CNRS, CEA Saclay, ICMMO and University Paris-Saclay for the financial support and analytical

Research Article
doi.org/10.1002/ejic.202400318

support facility at ICMMO. A. Aukauloo thanks the Institut Universitaire de France for support.

Conflict of Interests

The authors declare no conflict of interest.

Data Availability Statement

The data that support the findings of this study are available in the supplementary material of this article.

Keywords: Carbon dioxide · Cobalt corrole · CO · Methanol · Electroreduction

[1] a) S. Ren, D. Joulié, D. Salvatore, K. Torbensen, M. Wang, M. Robert, C. P. Berlinguette, *Science* **2019**, *365*, 367–369; b) M. Wang, K. Torbensen, D. Salvatore, S. Ren, D. Joulié, F. Dumoulin, D. Mendoza, B. Lassalle-Kaiser, U. Işci, C. P. Berlinguette, M. Robert, *Nat. Commun.* **2019**, *10*, 3602; c) X. Peng, M. Zhang, H. Qin, J. Han, Y. Xu, W. Li, X.-P. Zhang, W. Zhang, U.-P. Apfel, R. Cao, *Angew. Chem., Int. Ed.* **2024**, *63*, e202401074; d) M. M. Roubelakis, D. K. Bediako, D. K. Dogutan, D. G. Nocera, *J. Porphyrins Phthalocyanines* **2021**, *25*, 714–723; e) S. L. Foster, S. I. P. Bakovic, R. D. Duda, S. Maheshwari, R. D. Milton, S. D. Minteer, M. J. Janik, J. N. Renner, L. F. Greenlee, *Nat. Catal.* **2018**, *1*, 490–500.

[2] a) D. Tan, B. Wulan, X. Cao, J. Zhang, *Nano Energy* **2021**, *89*, 106460; b) J. Yin, Z. Yin, J. Jin, M. Sun, B. Huang, H. Lin, Z. Ma, M. Muzzio, M. Shen, C. Yu, H. Zhang, Y. Peng, P. Xi, C.-H. Yan, S. Sun, *J. Am. Chem. Soc.* **2021**, *143*, 15335–15343; c) X. Zhang, J. Li, Y.-Y. Li, Y. Jung, Y. Kuang, G. Zhu, Y. Liang, H. Dai, *J. Am. Chem. Soc.* **2021**, *143*, 3245–3255.

[3] a) M. Bernal, A. Bagger, F. Scholten, I. Sinev, A. Bergmann, M. Ahmadi, J. Rossmeisl, B. R. Cuenya, *Nano Energy* **2018**, *53*, 27–36; b) D. Gao, H. P. Wei, H. Li, L. Lin, G. Wang, X. Bao, *Acta Phys.-Chim. Sin.* **2021**, *37*, 2009021; c) D. Gao, H. Zhou, F. Cai, D. Wang, Y. Hu, B. Jiang, W.-B. Cai, X. Chen, R. Si, F. Yang, S. Miao, J. Wang, G. Wang, X. Bao, *Nano Res.* **2017**, *10*, 2181–2191; d) D. Ren, J. Gao, S. M. Zakeeruddin, M. Grätzel, *J. Phys. Chem. Lett.* **2021**, *12*, 7583–7589.

[4] a) C. Costentin, S. Drouet, M. Robert, J.-M. Savéant, *Science* **2012**, *338*, 90–94; b) C. Costentin, M. Robert, J.-M. Savéant, *Acc. Chem. Res.* **2015**, *48*, 2996–3006; c) P. De La Torre, J. S. Derrick, A. Snider, P. T. Smith, M. Loipersberger, M. Head-Gordon, C. J. Chang, *ACS Catalysis* **2022**, *12*, 8484–8493; d) M. R. Narouz, P. De La Torre, L. An, C. J. Chang, *Angew. Chem., Int. Ed.* **2022**, *61*, e202207666; e) C. G. Margarit, N. G. Asimow, M. I. Gonzalez, D. G. Nocera, *J. Phys. Chem. Lett.* **2020**, *11*, 1890–1895; f) J. Zheng, D. Zhou, J. Han, J. Liu, R. Cao, H. Lei, H. Bian, Y. Fang, *J. Phys. Chem. Lett.* **2022**, *13*, 11811–11817.

[5] a) C. Zhang, P. Gotico, R. Guillot, D. Dragoe, W. Leibl, Z. Halime, A. Aukauloo, *Angew. Chem., Int. Ed.* **2023**, *62*, e202214665; b) J. S. Derrick, M. Loipersberger, S. K. Nistanaki, A. V. Rothweiler, M. Head-Gordon, E. M. Nichols, C. J. Chang, *J. Am. Chem. Soc.* **2022**, *144*, 11656–11663.

[6] a) Y. Y. Birdja, J. Shen, M. T. M. Koper, *Catal. Today* **2017**, *288*, 37–47; b) M.-J. Cheng, Y. Kwon, M. Head-Gordon, A. T. Bell, *J. Phys. Chem. C* **2015**, *119*, 21345–21352.

[7] a) E. Boutin, M. Wang, J. C. Lin, M. Mesnage, D. Mendoza, B. Lassalle-Kaiser, C. Hahn, T. F. Jaramillo, M. Robert, *Angew. Chem., Int. Ed.* **2019**, *58*, 16172–16176; b) Y. Wu, G. Hu, C. L. Rooney, G. W. Brudvig, H. Wang, *ChemSusChem* **2020**, *13*, 6296–6299; c) Y. Wu, Z. Jiang, X. Lu, Y. Liang, H. Wang, *Nature* **2019**, *575*, 639–642.

[8] a) Z. Weng, Y. Wu, M. Wang, J. Jiang, K. Yang, S. Huo, X.-F. Wang, Q. Ma, G. W. Brudvig, V. S. Batista, Y. Liang, Z. Feng, H. Wang, *Nat. Commun.* **2018**, *9*, 415; b) J. Shen, R. Kortlever, R. Kas, Y. Y. Birdja, O. Diaz-Morales, Y. Kwon, I. Ledezma-Yanez, K. J. P. Schouten, G. Mul, M. T. M. Koper, *Nat. Commun.* **2015**, *6*, 8177.

[9] P. Gotico, B. Boitrel, R. Guillot, M. Sircoglou, A. Quaranta, Z. Halime, W. Leibl, A. Aukauloo, *Angew. Chem. Int. Ed.* **2019**, *58*, 4504–4509.

[10] a) S. Gonglach, S. Paul, M. Haas, F. Pillwein, S. S. Sreejith, S. Barman, R. De, S. Müllegger, P. Gerschel, U.-P. Apfel, H. Coskun, A. Aljabour, P. Stadler, W. Schöfberger, S. Roy, *Nat. Commun.* **2019**, *10*, 3864; b) J. Grodkowski, P. Neta, E. Fujita, A. Mahammed, L. Simkhovich, Z. Gross, *J. Phys. Chem. A* **2002**, *106*, 4772–4778.

[11] A. Khadhraoui, P. Gotico, B. Boitrel, W. Leibl, Z. Halime, A. Aukauloo, *Chem. Commun.* **2018**, *54*, 11630–11633.

[12] R. De, S. Gonglach, S. Paul, M. Haas, S. S. Sreejith, P. Gerschel, U.-P. Apfel, T. H. Vuong, J. Rabeah, S. Roy, W. Schöfberger, *Angew. Chem. Int. Ed.* **2020**, *59*, 10527–10534.

[13] W. Sinha, A. Mahammed, N. Fridman, Y. Diskin-Posner, L. J. W. Shimon, Z. Gross, *Chem. Commun.* **2019**, *55*, 11912–11915.

[14] a) A. Mahammed, I. Giladi, I. Goldberg, Z. Gross, *Chemistry – A European Journal* **2001**, *7*, 4259–4265; b) Z. Gross, G. Golubkov, L. Simkhovich, *Angew. Chem. Int. Ed.* **2000**, *39*, 4045–4047.

[15] P.-G. Julliard, S. Pascal, O. Siri, M. Giorgi, D. Cortés-Arriagada, L. Sanhueza, G. Canard, *Org. Biomol. Chem.* **2024**, *22*, 1993–1997.

[16] B. Wan, F. Cheng, J. Lan, Y. Zhao, G. Yang, Y.-M. Sun, L.-P. Si, H.-Y. Liu, *Int. J. Hydrog. Energy* **2023**, *48*, 5506–5517.

[17] C. Zhang, E. Prignot, O. Jeannin, A. Vacher, D. Dragoe, F. Camerel, Z. Halime, R. Gramage-Doria, *ACS Catal.* **2023**, *13*, 2367–2373.

[18] a) B. Hu, B. Chu, H. Cao, Z. Lei, S. Cui, P. Wang, J. Tang, X. Wang, B. Xu, *Chem Catal.* **2024**, *4*, 101014; b) Y. Song, P. Guo, T. Ma, J. Su, L. Huang, W. Guo, Y. Liu, G. Li, Y. Xin, Q. Zhang, S. Zhang, H. Shen, X. Feng, D. Yang, J. Tian, S. K. Ravi, B. Z. Tang, R. Ye, *Adv. Mater.* **2024**, *36*, 2310037.

[19] S. Brandès, V. Quesneau, O. Fonquernie, N. Desbois, V. Blondeau-Patissier, C. P. Gros, *Dalton Trans.* **2019**, *48*, 11651–11662.

[20] E. Boutin, A. Salamé, M. Robert, *Nat. Commun.* **2022**, *13*, 4190.

[21] M. Schmid, M. Zugermeier, J. Herritsch, B. P. Klein, C. K. Krug, L. Ruppenthal, P. Müller, M. Kothe, P. Schweyen, M. Bröring, J. M. Gottfried, *J. Phys. Chem. C* **2018**, *122*, 10392–10399.

[22] R. Yamuna, S. Ramakrishnan, K. Dhara, R. Devi, N. K. Kothurkar, E. Kirubha, P. K. Palanisamy, *J. Nanopart. Res.* **2013**, *15*, 1399.

Manuscript received: May 30, 2024
Revised manuscript received: June 28, 2024
Accepted manuscript online: July 3, 2024
Version of record online: August 30, 2024